Chemical and Process Engineering 2011, 32 (4), 351-366
DOI: 10.2478/v10176-011-0028-0

# NUMERICAL STUDY OF FLUID FLOW AND POWER CONSUMPTION IN A STIRRED VESSEL WITH A SCABA 6SRGT IMPELLER

Houari Ameur*, Mohamed Bouzit and Mustapha Helmaoui

Faculté de Génie Mécanique, USTO-MB, 1505 El M'nouar, Oran, Algérie

The present work deals with agitation of non-Newtonian fluids in a stirred vessel by Scaba impellers. A commercial CFD package (CFX 12.0) was used to solve the 3D hydrodynamics and to characterise at every point flow patterns especially in the region swept by the impeller. A shear thinning fluid with yield stress was modelled. The influence of agitator speed, impeller location and blade size on the fluid flow and power consumption was investigated. The results obtained are compared with available experimental data and a good agreement is observed. It was found that an increase in blade size is beneficial to enlargement of the well stirred region, but that results in an increased power consumption. A short distance between the impeller and the tank walls limits the flow around the agitator and yields higher power consumption. Thus, the precise middle of the tank is the most appropriate position for this kind of impeller.

**Keywords:** 3D numerical study, non-Newtonian fluid, stirred vessel, Scaba impeller, impeller eccentricity

## 1. INTRODUCTION

Mechanically stirred vessels are commonly used in the chemical, biochemical, food, mineral, polymer and pharmaceutical industries. The optimum design of a stirred tank for minimum capital and running costs depends on the desired production rate with a specified product's properties and it is achieved by, for example, a correct choice of tank and impeller geometry, rotational speed and location, of fluid addition and subtraction. A detailed knowledge of power and velocity distribution of the stirred tank configurations is therefore required.

In general, stirred vessels have been evaluated over the years through experimental investigations of a number of different impellers, vessel geometries, and fluid rheology. Such an approach is usually costly and sometimes it is not an easy task. With computational fluid dynamics (CFD), we can examine various parameters contributing to various phenomena in a shorter time and with less expense, a task otherwise difficult in experimental techniques. During the last two decades, CFD has become an important tool for understanding flow phenomena (Armenante et al., 1997), developing of new processes, and optimising the existing processes (Sahu et al., 1998). The capability of CFD tools to forecast mixing behaviour in terms of mixing time, power consumption, flow pattern and velocity profiles is considered as a successful achievement of these methods and acceptable results have been obtained. Kelly and Humphrey (1998) developed a CFD model for a large fermentor equipped with hydrofoil impellers and investigated the effect of the impeller speed and the fluid rheology on the flow near the perimeter of the fermentor. Murthy and Jayanti (2003) studied mixing of power-law fluids with an anchor impeller using CFD modelling. They verified the proportionality between the shear rate near the impeller and the rotational speed. They also showed that this proportionality constant is broadly

*Corresponding author, e-mail: houari_ameur@yahoo.fr

independent of the geometric and rheological properties of the mixing system. Iranshahi et al. (2006) investigated flow and mixing in a vessel equipped with a Paravisc impeller in the laminar regime. CFD techniques were applied to study the evolution of mixing patterns and predict the intensity of segregation, mixing time, mixing efficiency and pumping capability, and the results were compared with those obtained for conventional viscous mixing impellers, i.e., an anchor and double helical ribbon. Arratia et al. (2006) presented an experimental and numerical investigation of mixing in shear-thinning fluids with yield stress in stirred tanks. The numerical simulations captured the essential features of flow such as cavern formation and cavern–cavern segregation for a multiple impeller system. They found that mixing of shear-thinning yield stress fluids is controlled by chaotic flow: lobe formation, stretching, folding, and self-similar mixing patterns. To develop a model for aerated fermenters, Moilanen et al. (2006) combined gas–liquid mass transfer, bioreaction kinetics, and fluid rheology with computational fluid dynamics. They reported that their CFD model can be used for troubleshooting, design, and scale-up of aerobic fermenters.

A CFD model of a cylindrical pulp mixing chest equipped with a side-entering axial-flow A-310 impeller was developed by Saeed et al. (2007). They studied the effect of operating conditions and design parameters on cavern formation, mixing time, and velocity profiles generated by the impeller. Using CFD and ultrasonic Doppler velocimetry, Ihejirika and Ein-Mozaffari (2007) studied the effect of impeller speed, power, yield stress, and impeller pumping direction on the mixing performance of a helical ribbon impeller agitated in a non-Newtonian fluid. With CFD modeling and experiments, Couerbe, et al. (2008) illustrated the impact of thixotropy on flow patterns in a stirred tank. Ein-Mozaffari and Upreti, (2009), also Prajapati and Ein-Mozaffari (2009) were interested in mixing of yield stress fluid by an anchor impeller. Bhole (2009) has used CFD to model hydrodynamics of two axial flow impellers, using a Bingham approximation to describe pulp fibre suspension rheology; the impellers operated in the laminar and transition-to-turbulence regimes. Xia et al. (2009) studied trough numerical simulation and experimentation the hydrodynamic of shear thinning fluid in three bioreactors equipped with different impeller combinations. Down-pumping propeller (DPP), 6-curved-blade disc turbine (6CBDT) and 6-arrowy-blade disc turbine (6ABDT) were combined to form different impeller combinations. Gomez et al. (2010) and Vishalkumar et al. (2011) studied mixing of yield stress fluid in a stirred tank. Liang et al. (2011) have employed CFD to study mixing performance in high solid anaerobic digester (HSAD) with A-310 impeller and helical ribbon. They constructed a mathematical model to assess flow fields. Derksen (2009, 2011) has outlined procedures for detailed simulations of flow of viscous thixotropic liquids. Wu (2011) has evaluated six turbulence models for mechanical agitation of non-Newtonian fluids in a lab-scale anaerobic digestion tank with a pitched blade turbine (PBT) impeller. An alternative method to calculate the Reynolds number for the moving zone that characterises impeller rotation has been proposed to judge the flow regime.

Additional difficulties for optimisation of processes often occur with non-Newtonian fluids. In fact, hydrodynamics strongly depends on the nature of fluids involved in a stirred system. Viscoplastic fluids (also called yield stress fluids) are an important class of non-Newtonian fluids. These fluids flow only when the shear stress is above a certain threshold, the yield stress, and this leads in particular to dead zones in the flow which lower mixing efficiency (Anne-Archard et al., 2006; Fuente et al., 1997). Agitation of such fluids as Xanthan gum solution results in the formation of a zone of intense motion around the impeller (the so called cavern) with essentially stagnant and/or slow moving fluids elsewhere (Pakzad et al., 2007). The prediction of cavern size is important in the agitation of shear thinning fluids with yield stress, so one can be sure that the whole fluid is in motion and there is no undesirable poorly stirred region in the tank. For instance, when stagnant zones exist, poor heat and mass transfer rates, high temperature gradients, and if aerated, the possibility of oxygen starvation during fermentation will occur (Elson, 1990). Thus, it is desirable to eliminate these stagnant regions by properly designing and operating agitation systems.

The term cavern was first used by Wichterle and Wein (1975) to describe the moved zone around the impeller in extremely shear thinning suspensions of finely divided particulate solids.

Some work has been conducted using curved blade impellers to evaluate cavern size as a function of the power drawn by yield stress fluids including those by Galindo and Nienow (1992, 1993) for Lightnin A315 and Scaba 6SRGT impellers; (Amanullah et al., 1997) for axial flow SCABA 3SHPI impeller; (Serrando-Carreon and Galindo, 1997) for four different impellers (Rushton turbine, Chemineer He-3, CD-6 and Scaba 6SRGT) in individual and dual arrangements, (Pakzad et al., 2007, 2008) for SCABA 6SRGT impellers.

A thorough search of the literature suggests that little space has been devoted to numerical simulation of the agitation of yield stress fluid with Scaba 6SRGT impellers. Therefore, the objective of the present paper is to employ advanced computational fluid dynamics (CFD) to study flow patterns and power consumption for stirring shear thinning fluids possessing yield stress with this type of impellers. Our attention is focused on the effect of the Reynolds number, impeller clearance from the tank bottom, impeller eccentricity and the blade size (height and diameter).

## 2. DESCRIPTION OF THE STIRRED SYSTEM

The system consists of a cylindrical tank with a flat bottom (Fig. 1), the liquid level $H$ is equal to the diameter vessel $D$, with $D$ = 400 mm (Table 1). The impeller consists of six curved blades fixed on a disc with 8 mm of thickness, which is attached on a cylindrical central shaft of diameter $d_s/D$ = 0.05. All results are presented in dimensionless values, which enable the user to investigate any size of vessels. In this paper, different geometrical configurations are realized in order to test the effect of the impeller's location and blade size (Table 2).

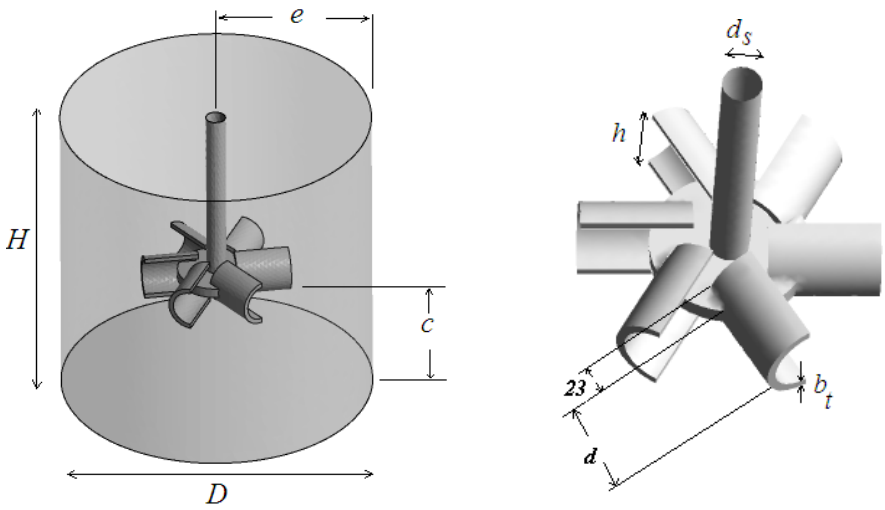


Fig. 1. Stirred system

Table 1. Vessel parameters

| | $D$ | $H$ | $d_s$ | $d_t$ | $b_t$ |
|---|---|---|---|---|---|
| [mm] | 400 | 400 | 20 | 8 | 6 |

Table 2. Parameters of all geometrical configurations realized

| *c/D* | *e/D* | *h/D* | *d/D* |
|---|---|---|---|
| 0.425 | 0 | 0.12 | 0.315 |
| | | | 0.440 |
| | | | 0.565 |
| 0.425 | 0 | 0.06 | 0.440 |
| | | 0.12 | |
| | | 0.18 | |
| 0.425 | 0 | 0.12 | 0.315 |
| | 0.125 | | |
| | 0.2 | | |
| 0.150 | 0 | 0.12 | 0.315 |
| 0.125 | | | |
| 0.250 | | | |
| 0.550 | | | |

## 3. NUMERICAL ISSUES

The commercially available computer code (CFX 12.0) developed by AEA Technology, UK (ANSYS Inc., 2009), was used to simulate the steady state 3D flow field generated by a Scaba impeller in the laminar regime. CFX is a general purpose computer program using a finite volume method. The Navier-Stokes equations written in a rotating, cylindrical frame of references are solved. Because of the choice of a rotating frame, two terms are added to the equations: centrifugal and Coriolis accelerations. The equations are written in terms of velocity components and pressure. These variables are discretized on a grid of control volumes, which enables a more precise mass conservation, and a faster convergence to be obtained. A pressure-correction method of the type Semi-Implicit Method for Pressure- Linked Equations-Consistent (SIMPLEC) is used to affect pressure-velocity coupling.

Constant boundary conditions have been set respecting a rotating reference frame (RRF) approach. Here, the impeller is kept stationary and the flow is steady relative to the rotating frame, while the outer wall of the vessel is given an angular velocity equal and opposite to the velocity of the rotating frame. This approach can be employed due to the absence of baffles. The same RRF approach, often used for stirred vessels, has given accurate results for several different stirring systems (Aubin et al., 2000; Naude, 1998). The simplification of the stirring system where baffles have been removed is obviously independent of the CFD resolution and is only due to mixing and industrial considerations. In the case of agitated vessels involving baffles, computational flow could nonetheless have been easily achieved with an MRF (Naude, 1998) or sliding meshes approaches.

A pre-processor (ICEM CFD 12.0) was used to discretize the flow domain with a tetrahedral mesh (Fig. 2). An increased mesh density was used near the impeller and the tank walls in order to capture the boundary layer flow details. A sufficient amount of nodes that define the curvature of the blades was created on the impeller's edge, which resulted in a very refined mesh. Mesh tests were performed (Table 3) by verifying that additional cells did not change velocity magnitude in the regions of high velocity gradients around the impeller blades by more than 2.5%.

To verify the grid independency, the number of cells was increased by a factor of about 2 used by other researchers in CFD modelling of mixing processes (Buwa et al., 2006; Letellier et al., 2002). The original 3D mesh of the model had 99,123 computational cells. To verify the grid independency, the number of cells was increased from 99,123 cells to 198,246 cells. The additional cells changed the velocity magnitude in the regions of high velocity gradients and the impeller power number by more than 3%. Thus, the number of cells was changed from 198,246 cells to 396,492 cells. The additional cells did not change the velocity magnitude in the regions of high velocity gradients and impeller power number by more than 2.5%. Therefore, 198,246 cells were employed in this study.

Simulations were considered converged when the scaled residuals for each transport equation were below $10^{-7}$. The velocities had converged to a single value. Most simulations required about 2000 iterations for convergence. Computations were carried out using Pentium(R) Dual Core CPU 2.20 GHz with 2.0 GB of RAM and convergence was typically achieved after 4 – 6 h.

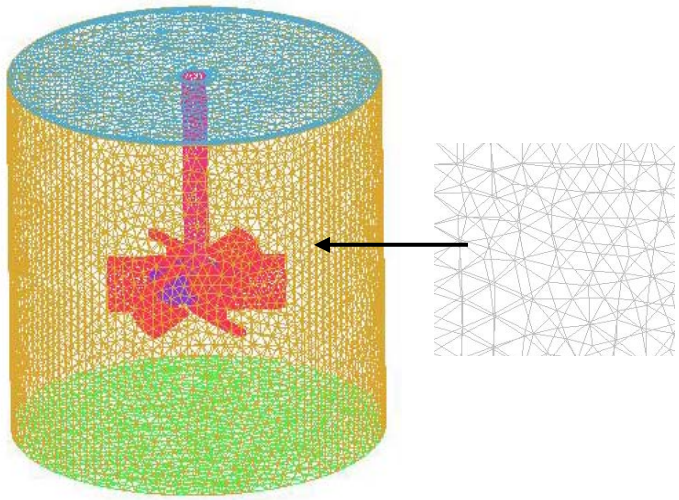

Fig. 2. Numerical grid (tetrahedral mesh)

Table 3. Details of mesh tests

| | M1 | M2 | M3 |
|---|---|---|---|
| Number of cells | 99123 | 198246 | 396492 |
| $V^*_{max}$ | 0.5105 | 0.5311 | 0.5366 |
| Time required [second] | 9263 | 16254 | 27586 |

## 4. THEORETICAL BACKGROUND

Shear thinning fluids with yield stress were modelled in this work, the Xanthan gum solution was considered. It's rheology can be described by the Herchel Bulkkley model (Macosko, 1994):

$$\tau = \tau_y + K\dot{\gamma}^n \tag{1}$$

Where $\tau_y$ is the yield stress, $K$ is the consistency index, $\dot{\gamma}$ is the shear rate and $n$ is the flow behaviour index.

According to the Metzner and Otto's correlation (Metzner and Otto, 1957), the average shear rate can be related to the impeller speed by:

$$\dot{\gamma}_{avg} = K_s N \tag{2}$$

The average shear rate can be used to evaluate the apparent viscosity ($\eta$) of the solution, which is a Herschel-Bulkley fluid.

$$\eta = \frac{\tau}{\dot{\gamma}_{avg}} = \frac{\tau}{k_s N} = \frac{\tau_y + K\left(K_s N\right)^n}{K_s N} \tag{3}$$

The Reynolds number can be given as:

$$Re_y = \frac{K_s N^2 D^2 \rho}{\tau_y + K\left(K_s N\right)^n} \tag{4}$$

Table 4 summarises the rheological properties of different Xanthan gum solutions used in this work, which are based on measurements conducted by Galindo and Nienow (1993).

Table 4. Rheological properties of Xanthan gum solutions

| Concentration [%] | $K$ [Pa s$^n$] | $n$ [-] | $\tau_y$ [Pa] |
|---|---|---|---|
| 1.5 | 14.5 | 0.12 | 7.1 |
| 3.5 | 33.1 | 0.18 | 20.6 |

The Hershel-Bulkley model causes numerical instability when the non-Newtonian viscosity blows up at small shear rates (Ford et al., 2006; Pakzad et al., 2008; Saeed et al., 2008). This problem is surmounted by the modified Hershel-Bulkley model given by:

$$\eta = \begin{cases} \eta_0 \quad for \quad \tau \le \tau_y \\ \dfrac{1}{\dot{\gamma}} \tau_y \, k \left( \dot{\gamma}^n - \left( \dfrac{\tau_y}{\eta_0} \right)^n \right) \quad for \quad \tau > \tau_y \end{cases} \tag{5}$$

Where $\eta_0$ is the yielding viscosity. The model considers the fluid to be very viscous with viscosity $\eta_0$ for shear stress $\tau \le \tau_y$ , and describes the fluid behaviour by a power law model for $\tau > \tau_y$.

The power consumption is a macroscopic result obtained by integration on the impeller surface of the local power transmitted by the impeller to the fluid. It is quite equivalent to say that the power consumption $P$ is entirely given by the impeller to the fluid (White, 1974). In these conditions:

$$P = \eta \int_{vessel\ volume} Q \, dv \tag{6}$$

The element $dv$ is written as:

$$dv = r \, dr \, d\theta \, dz \tag{7}$$

$$Q_v = \left(2\tau_{rr}^2 + 2\tau_{\theta\theta}^2 + 2\tau_{zz}^2 + \tau_{rz}^2 + \tau_{r\theta}^2 + \tau_{z\theta}^2\right) / \eta^2 \tag{8}$$

$$\tau_{rr} = -\eta \, 2 \partial v_r / \partial r \tag{9}$$

$$\tau_{r\theta} = -\eta\left[r\,\partial\left(v_\theta / r\right)/\partial r + \left(1/r\right)\partial v_r / \partial\theta\right] \tag{10}$$

$$\tau_{rz} = -\eta\left[\partial v_r / \partial z + \partial v_z / \partial r\right] \tag{11}$$

The power number is calculated according to this equation:

$$N_P = \frac{P}{\rho N^3 D^5} \tag{12}$$

## 5. RESULTS AND DISCUSSION

To validate the CFD model, the exactly similar geometrical conditions to those chosen by Pakzad et al. (2007) were considered, i.e. a baffled tank (Fig. 3). Predicted results for axial velocity profiles (Fig. 4) and power number (Fig. 5) were compared with the experimental data given by Pakzad: a satisfactory agreement is observed.

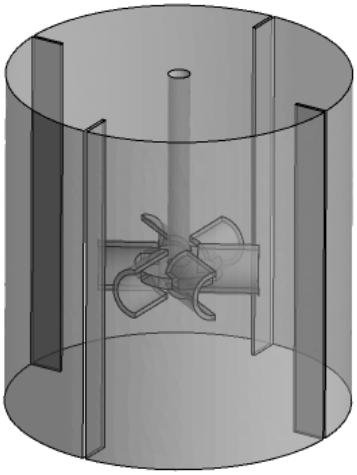

Fig. 3. Vessel configuration used for the validation

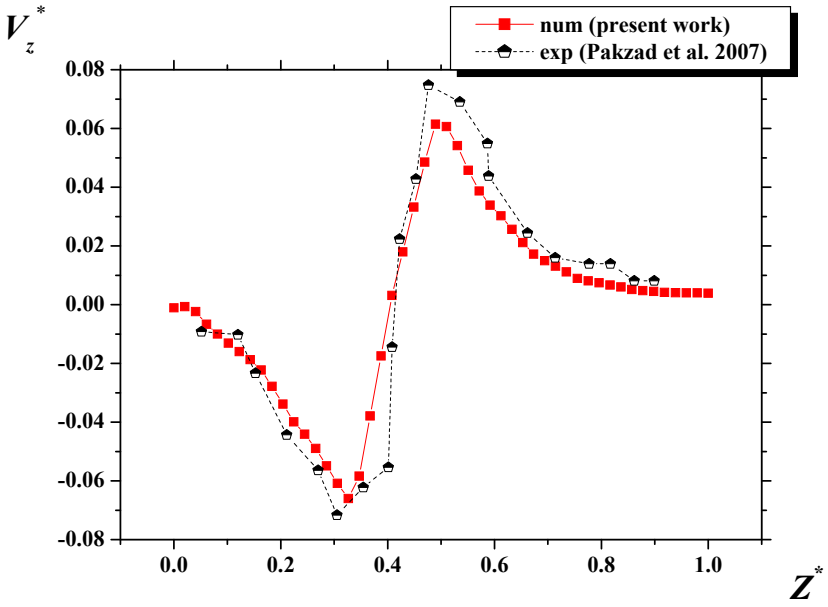


Fig. 4. Axial velocity for $Re_y = 80.9$, $n = 0.12$

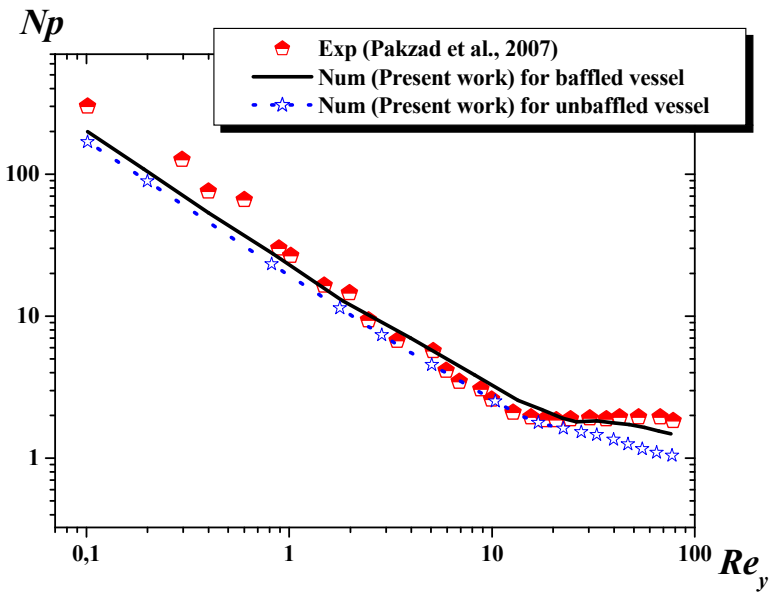


Fig. 5. Power number for $n$ = 0.12, $d/D$ = 0.315, $c/D$ = 0.425, $e/D$=0, $h/D$ = 0.12

In experimental studies, some errors can be marked and it may be due to the apparatus precision. We note that Pakzad et al. have presented in their paper a comparison between the experimental data and CFD results (for the velocity field and power consumption), and they have found a good agreement.

In the section that follows, the hydrodynamics of an unbaffled vessel stirred with a Scaba impeller located either coaxially or eccentrically is investigated. For mixing very viscous materials or when fouling on the vessel internals is to be limited, unbaffled vessels are sometimes used in industrial practice, eccentric configurations have been even less studied, but probably they have a wider practical interest. A review on the modelling of unbaffled stirred vessels can be found in (Galletti et al., 2008; 2009).

### *5.1. Effect of the Reynolds number*

When stagnant zones exist in a stirred vessel, poor heat and mass transfer rates, high temperature gradients, and if aerated, the possibility of oxygen starvation during fermentation will occur, thus it is necessary to eliminate the undesirable poor mixing regions in the tank (Pakzad et al., 2007).

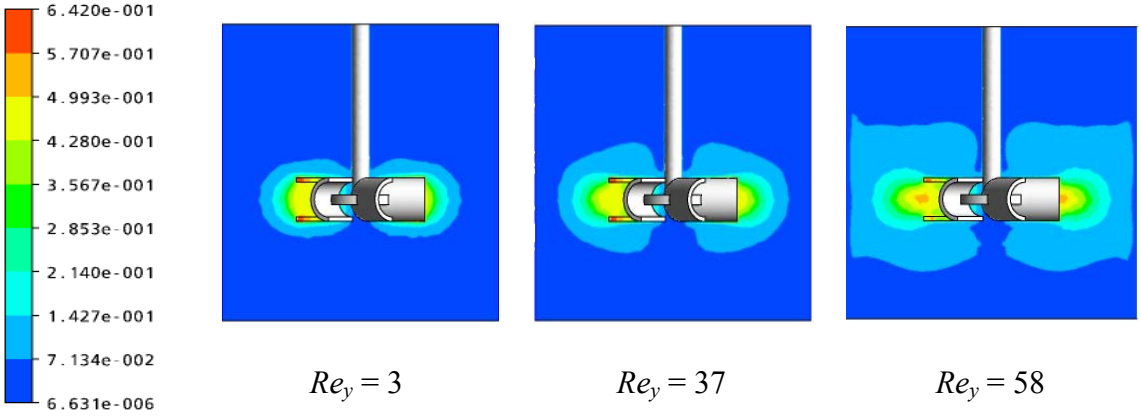


Fig. 6. Velocity magnitude contours for $n$ = 0.12, $d/D$ = 0.315, $c/D$ = 0.425, $h/D$ = 0.12

In the following, we present the effect of parameters on the flow fields. Fig. 6 illustrates various flow structures obtained for a Xanthan gun solution with 1.5% of mass concentration, at various stirring velocities. Generally, we observe a zone of flow repression; the liquid is pumped from the impeller to the vessel walls. For a small Reynolds number, the flow is almost radial and mainly limited to the central part of the tank. The velocity vectors measured close to the walls are almost negligible. For a more significant Reynolds number, the outgoing flow from the blades becomes larger.

### *5.2. Effect of impeller clearance from bottom of the tank*

The ongoing demand for improved impeller designs usually comes from users of industrial mixing equipment when vessels are to be designed for new plants or improvement is sought for existing designs or to enhance quality, capacity, process efficiency and energy efficiency. For meeting these objectives, it is imperative that the relationship between the flow pattern and the design objective is understood. One of the flow characteristics affecting the impeller flow efficiency is the presence of trailing vortices generated at the tip of the impeller blades.

Predicted vectors of flow generated by the Scaba 6SRGT at $Re_y = 60$ in the vertical plane aligned with the impeller shaft are presented in Fig. 7. The plots show two circulating loops, one below and one above the impeller. As expected the flow pattern generated by the Scaba impeller is similar to those produced by the typical radial flow impellers.

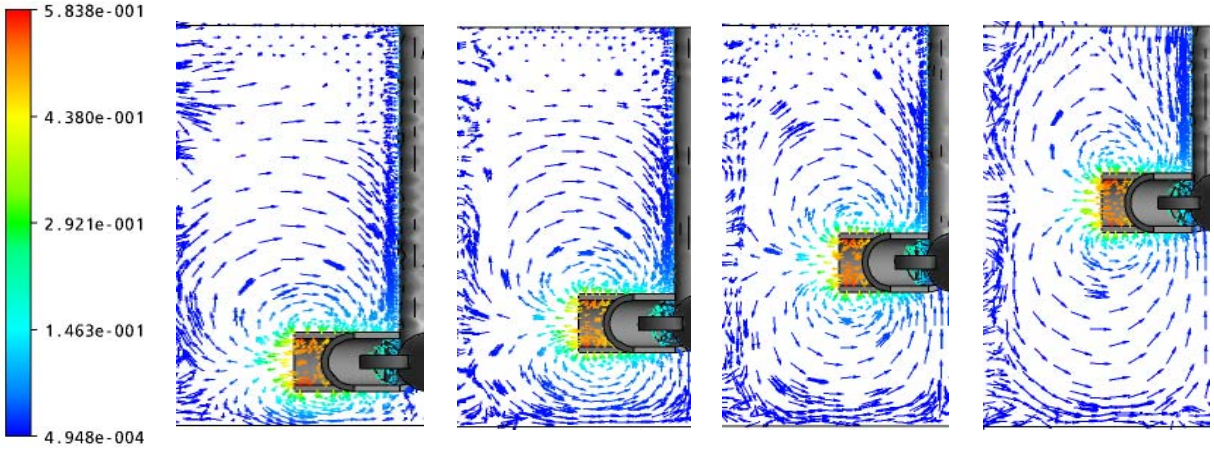


Fig. 7. Velocity vectors for $Re_y = 60$, $n = 0.18$, $d/D = 0.315$, $h/D = 0.12$

It is shown that increased impeller clearance from the vessel base is beneficial for generating larger cavern volumes for a given power input.

At a radial location $R^* = 2R/D = 0.8$, and in dimensionless form reported to the impeller tip velocity $\pi ND$; the profiles are independent of the impeller clearance from bottom of the tank (Fig. 8). The axial velocity becomes negligible in the top half of the tank when the impeller is placed near the bottom of the tank ($c/D = 0.150$). When the stirrer is positioned above the middle of the vessel, the lower part is not disturbed. These results are confirmed by Fig. 6, where the flow fields are illustrated for the four geometric configurations. If the impeller is located closer to the bottom of the tank, increased viscous resistance occurs, which limits the flow around the agitator, which leads to a high power consumption. Thus, the exact middle of the tank is the most appropriate position for this type of mixer and for this range of Reynolds numbers.

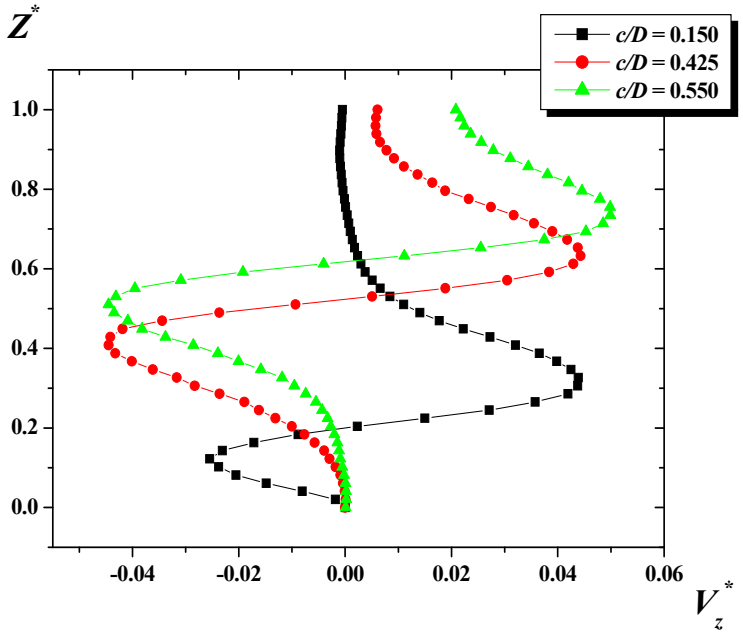


Fig. 8. Axial velocity profiles for $Re_y = 80$, $n = 0.18$, $R^* = 0.8$, $d/D = 0.315$, $h/D = 0.12$

Table 5. Power number for different vertical positions of impeller ($c/D$), with $n = 0.18$, $e/D = 0$, $d/D = 0.315$, $h/D = 0.2$

| $Re_y$ | $c/D = 0.150$ | $c/D = 0.250$ | $c/D = 0.425$ | $c/D = 0.550$ |
|---|---|---|---|---|
| 0.1 | 170.714 | 168.088 | 165.481 | 164.015 |
| 1 | 17.203 | 16.928 | 16.675 | 16.540 |
| 10 | 1.798 | 1.765 | 1.743 | 1.734 |

Power consumption constitutes a global parameter to describe performance of a mechanically stirred system. Fig. 5 represents the variations of $Np$ versus of $Re_y$ in a logarithmic scale. It can be seen that at Reynolds numbers less than 10 the line with the slope of −1 fits the data quite well. In the transitional regime, the power number changes slightly with $Re_y$. The confrontation of our results with those from the literature shows a good agreement.

For more details about parameters influencing power consumption, different tests have been performed concerning geometrical conditions. . The results of these tests are summarised in Table 5. The results obtained, confirm the conclusion drawn previously that the proximity of the impeller to the walls generates an increase in the power drawn.

### *5.3. Effect of impeller eccentricity*

Different horizontal locations of the impeller are realized in order to test the wall effect on the flow induced. The impeller eccentricity presents an extreme importance on the elimination of dead zones (Fig. 9), by consequence on the power requested (Fig. 10). With long distance from the centre of the tank, shear stress becomes more intense and a trailing vortex develops behind the wasteful blade of energy. The size of vortex and the power consumption increase proportionally with the ratio ($e/D$).

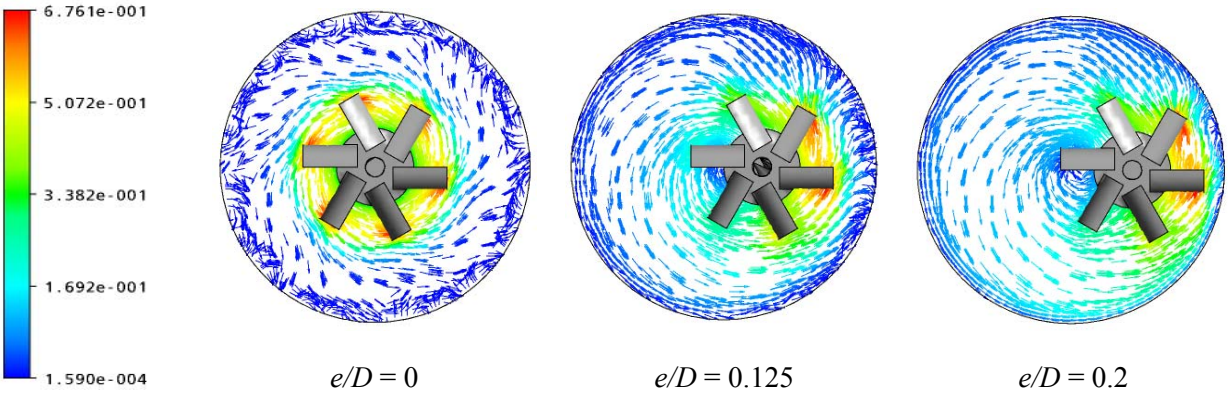


Fig. 9. Velocity vectors for $n = 0.18$, $c/D = 0.425$, $Re_y = 50$, $d/D = 0.315$, $h/D = 0.12$

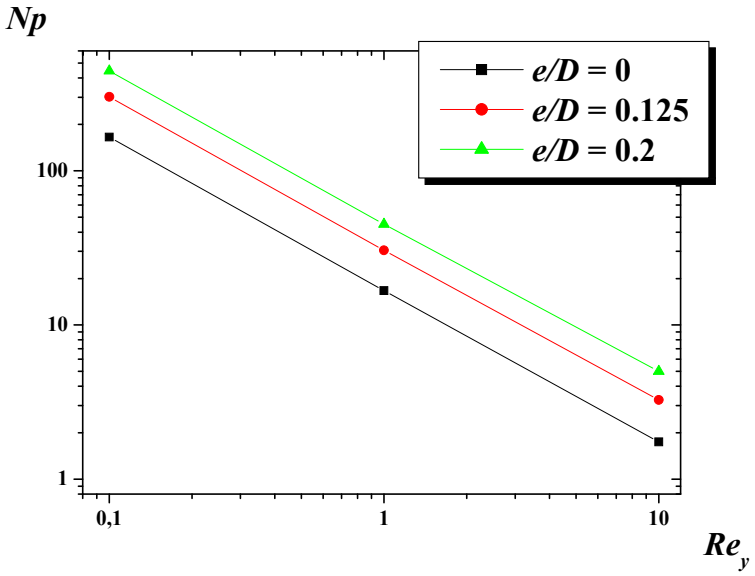


Fig. 10. Power number for $n = 0.18$, $c/D = 0.425$, $d/D = 0.315$, $h/D = 0.12$

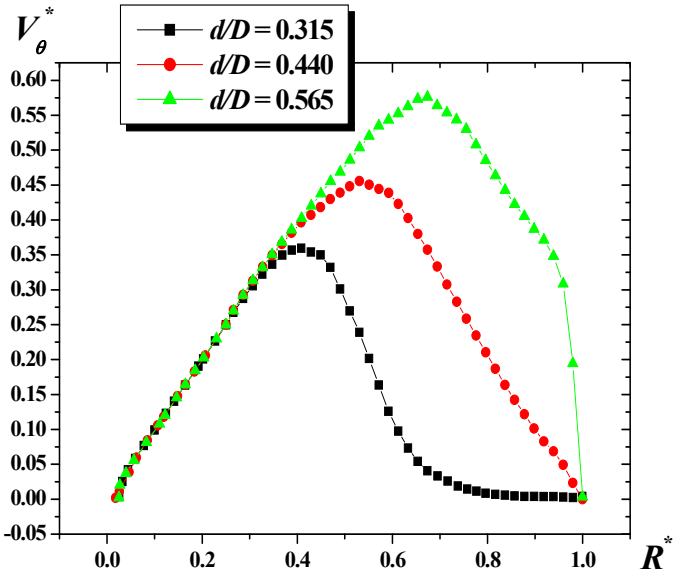


Fig. 11. Tangential velocity for $n = 0.18$, $c/D = 0.425$, $Re_y = 17$, $h/D = 0.12$

### 5.4. Effect of blade diameter

The influence of the impeller's diameter in the tank is studied in the case of $c/D$ = 0.425, $h/D$ = 0.12 and $e/D$ = 0. As illustrated in Fig. 11, the vicinity of the blade diameter leads to a great increase in the intensity of the fluid flows, and the cavern size becomes larger (Fig. 12), but it requires more power consumption (Fig. 13).

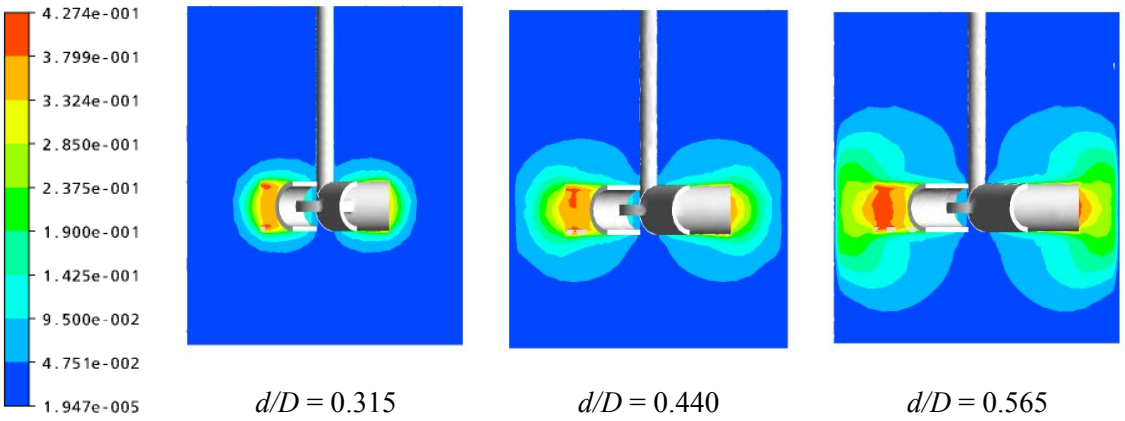


Fig. 12. Velocity contours for $n$ = 0.18, $c/D$ = 0.425, $Re_y$ = 17, $h/D$ = 0.12

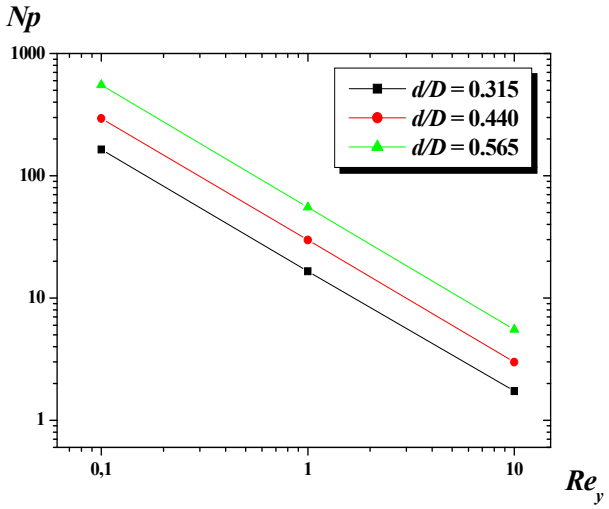


Fig. 13. Power consumption for $n$ = 0.18, $e/D$ = 0, $c/D$ = 0.250, $h/D$ = 0.12

### 5.5. Effect of blade height

The effect of blade height on the flow patterns and power consumption has also been studied. To perform this test, three geometrical configurations have been realized, which are: $h/D$ = 0.06, 0.12 and 0.18.

The variations of radial velocity component along the vessel height and for different height ratio of blade are plotted in Fig. 14. We can add that the radial flow impinging from the impeller becomes more significant with an increase in blade height.

The area swept by the impeller becomes greater with an increase in blade height, the cavern size is then larger (Fig. 15), but the required power consumption becomes more significant when the Reynolds number and the structural index remain the same (Fig. 16).

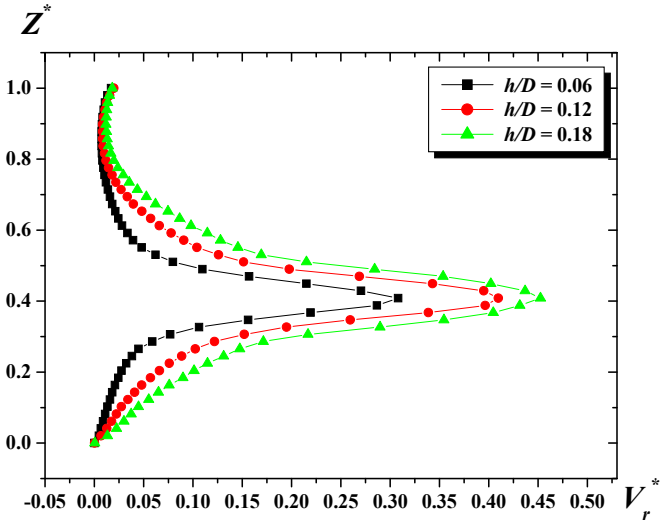


Fig. 14. Radial velocity for $n = 0.18$, $c/D = 0.425$, $Re_y = 40$, $d/D = 0.44$

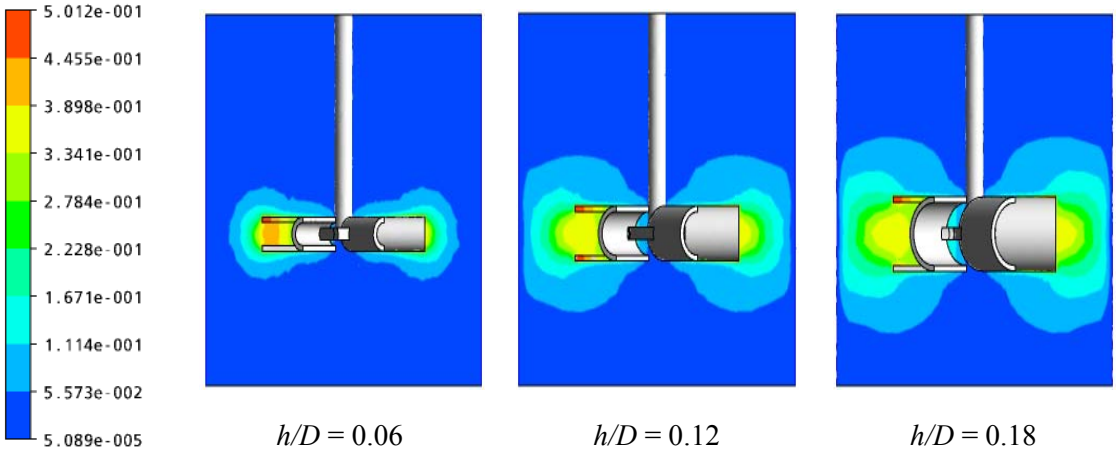


Fig. 15. Velocity magnitude contours for $n = 0.18$, $c/D = 0.425$, $Re_y = 40$, $d/D = 0.44$

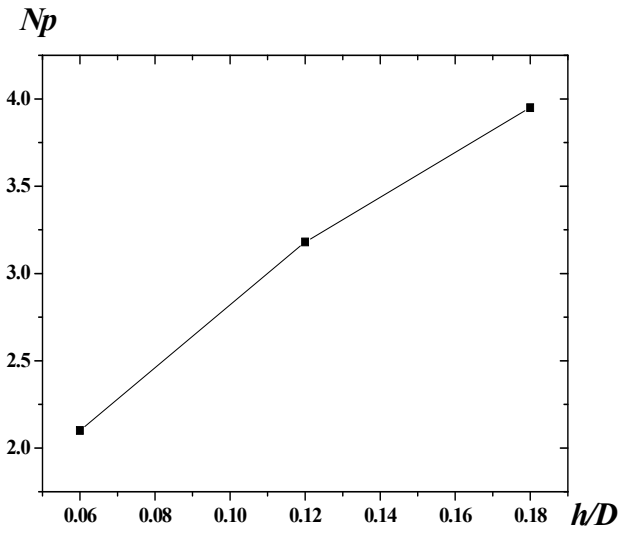


Fig. 16. Power number for $n = 0.18$, $c/D = 0.425$, $Re_y = 10$, $d/D = 0.44$

## 6. CONCLUSIONS

Computational fluid dynamics simulations were performed to determine the velocity fields and power consumption within a cylindrical tank equipped with a Scaba 6SRGT impeller in the agitation of Xanthan gum. First, it has to be noted that a good agreement is observed between these results and those available in the literature.

The effects of the impeller's location and blade size have been analysed. For the velocity profiles, the maximum is marked at the blade tip for any location of the impeller. If the impeller is located closer to the tank walls (bottom or side), increased viscous resistance occurs, which limits the flow around the agitator, which leads to a high power consumption. Thus, the exact middle of the tank is the most appropriate position for this kind of impeller and this range of Reynolds numbers. An increase in blade size is beneficial for the enlargement of the well stirred region, but that results in increased power consumption.

## SYMBOLS

| | |
|---|---|
| $b_t$ | blade thickness, m |
| $c$ | impeller off-bottomed clearance, m |
| $e$ | impeller eccentricity, m |
| $d$ | blade diameter, m |
| $d_s$ | shaft diameter, m |
| $d_t$ | disc thickness, m |
| $h$ | blade height , m |
| $n$ | flow behaviour index, dimensionless |
| $D$ | tank diameter, m |
| $H$ | liquid level, m |
| $K$ | consistency index, Pa $s^n$ |
| $K_s$ | Metzner-Otto's constant, dimensionless |
| $N$ | impeller rotational speed, 1/s |
| $P$ | power, W |
| $Np$ | power number, dimensionless |
| $Q_v$ | viscous dissipation function, $1/s^2$ |
| $R$ | radial coordinate, m |
| $Re$ | Reynolds number for a Newtonian fluid, dimensionless |
| $Re_y$ | Reynolds number for a yield stress fluid, dimensionless |
| $V$ | velocity, m/s |
| $V_z$ | axial velocity, m/s |
| $V_\theta$ | tangential velocity, m/s |
| $V_r$ | radial velocity, m/s |

*Greek symbols*

| | |
|---|---|
| $\dot{\gamma}_{avg}$ | average shear rate, 1/s |
| $\tau$ | shear stress, Pa |
| $\tau_y$ | suspension yield stress, Pa |
| $\rho$ | fluid density, $kg/m^3$ |
| $\eta$ | apparent viscosity, Pa s |
| $\eta_0$ | yielding viscosity, Pa s |
| $\theta$ | angular coordinate, degree |
| $\omega$ | angular velocity, rad/s |

## REFERENCES

Anne-Archard D., Marouche M., Boisson H.C., 2006. Hydrodynamics and Metzner–Otto correlation in stirred vessels for yield stress fluids. *Chem. Eng. J.,* 125, 15-24. DOI:10.1016/j.cej.2006.08.002.

Amanullah A., Hjorth S.A., Nienow A.W., 1997. Cavern sizes generated in highly shear thinning viscous fluids by Scaba 3SHP1 impeller. *Food Bioprod. Process,* 75, 232-238. DOI:10.1205/096030897531630.

Armenante P.M., Luo C., Chou C.C., Fort I., Medek J., 1997. Velocity profiles in a closed, unbaffled vessel: comparison between experimental LDV data and numerical CFD prediction. *Chem. Eng. Sci.,* 52, 3483-3492. DOI:10.1016/S0009-2509(97)00150-4.

Arratia P.E., Kukura J., Lacombe J., Muzzio F.J., 2006. Mixing of shear-thinning fluids with yield stress in stirred tanks. *AIChE J.,* 52, 2310-2322. DOI: 10.1002/aic.10847.

Aubin J., Naude I., Xuereb C., Bertrand J., 2000. Blending of Newtonian and shear-thinning fluids in a tank stirred with a helical screw agitator. *Trans. Inst. Chem. Eng.,* 78(A), 1105-1114. DOI : 10.1205/026387600528382.

Bhole M., Ford C., Bennington C.P.J., 2009. Characterization of axial flow impellers in pulp fibre suspensions. *Chem. Eng. Res. Des.,* 87, 648-653. DOI:10.1016/j.cherd.2008.11.002.

Buwa V., Dewan A., Nasser A.F., Durst F., 2006. Fluid dynamics and mixing of single-phase flow in a stirred vessel with a grid disc impeller: experimental and numerical investigations, *Chem. Eng. Sci*. 61, 2815-2822. DOI: 10.1016/j.ces.2005.10.066.

Couerbe G., Fletcher D.F., Xuereb C., Poux M., 2008. Impact of thixotropy on flow patterns induced in a stirred tank: Numerical and experimental studies. *Chem. Eng. Res. Des.,* 86, 545-553. DOI: 10.1016/j.cherd.2007.11.010.

Derksen J.J., Prashant A., 2009. Simulations of complex flow of thixotropic liquids. *J. Non-Newton. F. Mech.,* 160, 65-75. DOI:10.1016/j.jnnfm.2009.02.011.

Derksen J.J., 2011. Simulations of thixotropic liquids. *App. Math. Mod.,* 35, 1656-1665. DOI:10.1016/j.apm.2010.09.042.

Elson T.P., 1990. The growth of caverns formed around rotation impellers during the mixing of a yield stress fluid. *Chem. Eng. Commun.,* 96, 303-391. DOI:10.1080/00986449008911498.

Ein-Mozaffari F., Upreti S.R., 2009. Using electronic Dopller velocimetry and CFD modeling to investigate the mixing of non-Newtonian fluids possessing yield stress. *Chem. Eng. Res. Des.,* 87, 515-523. DOI:10.1016/j.cherd.2008.12.020.

Ford C., Ein-Mozaffari F., Bennington C.P.J., Taghipour F., 2006. simulation of mixing dynamics in agitated pulp stock chests using CFD. *AIChE J*., 52 (10), 3562-3569. DOI: 10.1002/aic.10958.

Fuente B., Choplin L., Tanguy P. A., 1997. Mixing with helical ribbon impellers: effect of highly shear thinning behavior and impeller geometry. *Trans. I. Chem. Eng.,* 75, 45-52. DOI:10.1205/026387697523381.

Galindo E., Nienow A.W., 1992. Mixing of highly viscous simulated xanthan fermentation broths with the Lightnin A-315 impeller. *Biotechnol. Prog.,* 8, 233-239. DOI: 10.1021/bp00015a009.

Galindo E., Nienow A.W., 1993. The performance of the Scaba 6SRGT agitator in the mixing of simulated xanthan gum broths. *Chem. Eng. Technol.* 16, 102-108. DOI: 10.1002/ceat.270160206.

Gomez C., Derakhshandeh B., Hatzikiriakos S.G., Bennington C.P.J., 2010. Carbopol as a model fluid for studying mixing of pulp fibre suspensions. *Chem. Eng. Sci.,* 65, 1288-1295. DOI:10.1016/j.ces.2009.09.085.

Iranshahi A., Heniche M., Bertrand F., Tanguy P.A., 2006. Numerical investigation of the mixing efficiency of the Ekato Paravisc impeller. *Chem. Eng. Sci.,* 61, 2609-2617. DOI:10.1016/j.ces.2005.11.032.

Ihejirika P., Ein-Mozaffari F., 2007. Using CFD and ultrasonic velocimetry to study the mixing of pseudoplastic fluids with a helical ribbon impeller. *Chem. Eng. Technol.,* 30, 606-614. DOI: 10.1002/ceat.200700006.

Kelly W., Humphrey A.E., 1998. Computational fluid dynamics model for predicting flow of viscous fluids in a large fermentor with hydrofoil flow impellers and internal cooling coils, *Biotechnol. Prog.,* 14, 248-258. DOI: 10.1021/bp9701168.

Letellier B., Xuereb C., Swaels P., Hobbes P., Bertrand J., 2002. Scale-up in laminar and transient regimes of a multi-stage stirrer, a CFD approach, *Chem. Eng. Sci.,* 57, 4617 - 4632. DOI: S0009-2509(02)00371-8.

Liang Y., Jingwei M., Shulin C., 2011. Numerical simulation of mechanical mixing in high solid anaerobic digester. *Bioresource Tech.,* 102, 1012–1018. DOI:10.1016/j.biortech.2010.09.079.

Macosko C.W., 1994. *Rheology: Principles, Measurements & Applications*. Wiley-VCH, New York, 47-49.

Metzner B., Otto R.E., 1957. Agitation of non-Newtonian fluids. *AIChE J.,* 3, 3-11. DOI : 10.1016/S0065-2377(08)60311-7.

Moilanen P., Laakkonen M., Aittamaa J., 2006. Modeling aerated fermenters with CFD. *Ind. Eng. Chem. Res.,* 45, 8656-8663. DOI:10.1016/S1570-7946(05)80240-8.

Murthy S.S., Jayanti S., 2003. Mixing of power-law fluids using anchors: Metzner-Otto concept revisited. *AIChE J.,* 49, 30-40. DOI: 10.1002/aic.690490105.

Naude I., 1998. Direct simulations of impellers in a stirred tank. Contribution to the optimization of the choice of an agitator, *Ph.D. thesis,* INPT, France.

Pakzad L., Ein-Mozaffari F., Chan P., 2007. Using computational fluid dynamics modeling to study the mixing of pseudoplastic fluids with a Scaba 6SRGT impeller. *Chem. Eng. Proc.,* 47, 2218-2227. DOI:10.1016/j.cep.2007.12.003.

Pakzad L., Ein-Mozaffari F., Chan P., 2008. Using electrical resistance tomography and computational fluid dynamics modeling to study the formation of cavern in the mixing of pseudoplastic fluids possessing yield stress. *Chem. Eng. Sci.,* 63, 2508-2522. DOI:10.1016/j.ces.2008.02.009.

Prajapati P., Ein-Mozaffari F., 2009. CFD investigation of the mixing of yield-pseudoplastic fluids with anchor impeller. *Chem. Eng. Tech.,* 32, 1211-1218. DOI: 10.1002/ceat.200800511.

Saeed S., Ein-Mozaffari F., Upreti S.R., 2007. Using computational fluid dynamics modeling and ultrasonic doppler velocimetry to study pulp suspension mixing. *Ind. Eng. Chem. Res.,* 46, 2172-2179. DOI: 10.1021/ie0607548.

Saeed S., Ein-Mozaffari F., 2008. Using dynamic tests to study the continuous mixing of xanthan gum solutions. *J. Chem. Technol. Biotechnol*., 83 (4), 559-568. DOI: 10.1002/jctb.1833.

Sahu A.K., Kummar P., Joshi J.B., 1998. Simulation of flow in stirred vessels with axial flow impellers: zonal modeling and optimization of parameter. *Ind. Eng. Chem. Res.,* 37, 2116-2130. DOI: 10.1021/ie970321s.

Serrano-Carreon L., Galindo E., 1997. Studies on cavern development in mixing a yield stress fluid in a pilot-scale Proto-Fermenter, In: Villermaux J., Bertrand J. (Eds.), *Récents Progrès en Génie des Procédés*, 11, 161-168.

Singh H., Fletcher D.F., Nijdam J.J., 2011. An assessment of different turbulence models for predicting flow in a baffled tank stirred with a Rushton turbine. *Chem. Eng. Sci.*, 66, 5976-5988. DOI:10.1016/j.ces.2011.08.018.

Vishalkumar R.P., Ein-Mozaffari F., Upreti S.R., 2011. Effect of time delays in characterizing the continuous mixing of non-Newtonian fluids in stirred-tank reactors. *Chem. Eng. Res. Des.,* 89, 1919-1928. DOI: 10.1016/j.cherd.2011.01.023.

White F.M., 1974. *Viscous Fluid Flow*, McGraw-Hill, New York, USA, 62-64.

Wichterle K., Wein O., 1975. Agitation of concentrated suspensions. *CHISA,* B4.6, Prague, Czechoslovakia. 2-5 July 1975, 33-39.

Wu B., 2011. CFD investigation of turbulence models for mechanical agitation of non-Newtonian fluids in anaerobic digesters. *Water Res.,* 45, 2082-2094. DOI:10.1016/j.watres.2010.12.020.

www.ansys.com

Xia J.Y., Wang Y.H., Zhang S., Chen N., Yin P., Zhuang Y., Chu J., 2009. Fluid dynamics investigation of variant impeller combinations by simulation and fermentation experiment. *Biochem. Chem. Eng. J.,* 43, 252-260. DOI: 10.1016/j.bej.2008.10.010.

*Received 29 July 2011*
*Received in revised form 12 December 2011*
*Accepted 15 December 2011*